Multimethod determination of the below-cloud wet scavenging coefficients of aerosols in Beijing, China

Danhui Xu[1,2], Baozhu Ge[1,*], Xueshun Chen[1], Yele Sun[1], Nianliang Cheng[3], Mei Li[4,5], Xiaole Pan[1], Zhiqiang Ma[6], Yuepeng, Pan[1], Zifa Wang[1]

5   [1]State Key Laboratory of Atmospheric Boundary Layer Physics and Atmospheric Chemistry, Institute of Atmospheric Physics, Chinese Academy of Sciences, Beijing 100029, China
[2]University of Chinese Academy of Sciences, Beijing 100049, China
[3]Beijing Municipal Environmental Monitoring Center, Beijing 100048, China
[4]Institute of Mass Spectrometer and Atmospheric Environment, Jinan University, Guangzhou 510632, China
10 [5]Guangdong Provincial Engineering Research Center for on-line source apportionment system of air pollution, Guangzhou 510632, China
[6]Beijing Shangdianzi Regional Atmosphere Watch Station, Beijing 100089, China

Correspondence: gebz@mail.iap.ac.cn

15

Atmospheric
Chemistry
and Physics
Discussions
Open Access

EGU

Abstract. Wet scavenging is one of the most efficient processes that remove aerosols from the atmosphere. This process is not well constrained in chemical transport models (CTMs) due to a paucity of localized parameterization regarding below-cloud wet scavenging coefficient (BWSC). Here we conducted field measurements of the BWSC during the Atmospheric Pollution and Human Health-Beijing (APHH-Beijing) campaign of 2016. Notably, the observed BWSC values based on the updated aerosol mass balance agree well with another estimation technique by the updated aerosol mass balance, and they fall in a range of 10^{-5} s^{-1}. The measurement in this winter campaign, combined with that in summer of 2014, supported an exponential power distribution of BWSCs with rainfall intensity. The observed parameters were also compared with both the theoretical calculations and modeling results. We found that the theoretical estimations can effectively characterize the observed BWSCs of aerosols with size smaller than 0.2 μm and larger than 2.5 μm. However, the theoretical estimations were one magnitude lower than observed BWSCs within 0.2-2.5 μm, a domain size range of urban aerosols. Such an underestimation of BWSC through theoretical method has been confirmed not only in APHH-Beijing campaign but also in all the rainfall events in summer of 2014. Since the model calculations usually originated from the theoretical estimations with simplified scheme, the significant lower BWSC would well explain the underprediction of wet depositions in polluted regions as reported by the Model Inter-Comparison Study for Asia (MICS-Asia) and the global assessment of the Task Force on Hemispheric Transport of Atmospheric Pollutants (TF-HTAP). The findings highlighted that the wet deposition module in the CTMs requires improvement based on field measurement estimation to construct a more reasonable simulation scheme for BWSC, especially in polluted regions.

1 Introduction

Wet deposition is one of the dominant aerosol sinks on both global and regional scales (Min et al., 2005;Textor et al., 2006), and can be divided into in-cloud (particles are activated as cloud condensation nuclei and absorbed by cloud water) and below-cloud scavenging (aerosols and gas are captured by raindrops or snow particles after the hydrometeors leave the clouds) (Zhao et al., 2015). Previously, below-cloud scavenging is thought to be less important than in-cloud process and always simplified or even ignored in most global and regional chemical transport models (CTMs) (Tang et al., 2006;Bae et al., 2010;Barth et al., 2000;ENVIRON.Inc, 2005;Stier et al., 2005). This may be true in most clean atmosphere, e.g., developed country where air pollutants in the boundary layer were not sufficient. This may be not the case in polluted regions. Recently, regional model in MICS-Asia (Model Inter-Comparison Study for Asia) has found the obvious underestimation of wet deposition in East Asia (Wang et al., 2008). For global model assessment by Hemispheric Transport of Atmospheric Pollutants (TF-HTAP), wet depositions are also underpredicted in region of North America, Europe and Asia where measured the high level of volume weighted averaged (VWA) nitrogen (N) concentrations in rainfall as > 1.25 mg N L^{-1} (Vet et al., 2014). Besides the uncertainties in emission inventory and chemical mechanism, the below-cloud scavenging process may also contribute to certain effects on the wet deposition simulation (Wang et al., 2008). Actually, below-cloud scavenging cannot be negligible in

CTMs, which contributed to more than 53% of the total wet deposition in some polluted areas such as India (Chatterjee et al., 2010) and North China (Ge et al., 2016;Xu et al., 2017).

Extensive efforts have been focused on the study of wet scavenging, and many researchers have noted that precipitation, even light rain, can remove 50-80% of the number or mass concentration of below-cloud aerosols (Andronache, 2004b;Zhang et al., 2004). The below-cloud wet scavenging coefficient (hereafter, BWSC), denoted K or $K(d_p)$ for size-resolved values, is a parameter that describes scavenging ability characteristics fairly well. The main factors affecting the BWSC include raindrop number size distribution, collection efficiency and raindrop terminal velocity, remain un-known and hence make the large uncertainties of BWSC (Wang et al., 2010). Seinfeld and Pandis (1998) proposed that collection efficiency (Brownian diffusion, directional interception, inertial impaction, thermophoresis and diffusion electrophoresis) is critical in the below-cloud scavenging process. Coarse particles (aerosol particle sizes d_p ranging from 2-20 μm) are easily scavenged by inertial impaction. Especially coarse particles ($d_p > 20$ μm) are also easily scavenged through the effect of gravity. Fine particles ($d_p < 0.2$ μm) can be removed by Brownian diffusion. However, accumulation mode aerosols (0.2 μm $< d_p < 2$ μm) are neither efficiently scavenged by Brownian diffusion nor by directional interception or inertial impaction, and this particle size range is called the "Greenfield gap" (Slinn, 1984). Recently, Bae et al. (2010) added phoretic and electric charging effects to the collection efficiency assessment and found that the BWSCs increase by up to 20 times in the 0.2-3 μm particle size range. Wang et al. (2014c) also improved the understanding of the electrical effects of the collision efficiency, which is also assumed to be a major source of uncertainty but is always ignored in theoretical estimations. It also improved the BWSC estimation by an order of magnitude. The raindrop number size distribution and raindrop terminal velocity are both represented by empirical mathematical functions, and these factors are non-negligible. In order to minimize the computational burden, the calculation of BWSCs in most global and regional-scale models are expressed as the product of rain intensity multiplied by the collection efficiency, where the later is simplified as a constant or calculated based on the work of Slinn (Bae et al., 2010;Slinn, 1984). This simplification may undoubtedly bring into large uncertainties and make the simulated wet deposition within a factor of two ranges of the observations, which is significant larger compared with the 30% bias of the prediction of air pollutants evaluation (Vet et al., 2014;Zhu et al., 2018).

Over the past few decades, a lot of wet scavenging coefficient (WSC) field measurements have been the focus of a large number of studies (Andronache, 2004b;Jylhä, 1991;Laakso et al., 2003;Okita et al., 1996;Wang et al., 2014c;Xu et al., 2017). In their field measurements, Okita et al. (1996) used the precipitation intensity, cloud-base height and the ratio between the sulfate concentration in aerosols of air mass and in rainwater to estimate the WSC, and this method is widely applied in most field measurements at present (Andronache, 2004b;Yamagata et al., 2009). However, this method cannot distinguish the below cloud part from the whole wet scavenging process, which is important to the parameterization scheme in CTMs. Xu et al. (2017) adopted sequential sampling and estimated the BWSCs of various soluble inorganic ions using the washout fraction concentration. In addition, the BWSCs display a strong dependency on the aerosol particle size distribution. Laakso et al. (2003) indicated that the BWSCs could be calculated by the aerosol particle number concentrations for various size ranges

Atmospheric
Chemistry
and Physics
Discussions

80   both before and after rain. This size-resolved method was also applied in Lanzhou (Zhao et al., 2015), Huang Mountain (Wang
       et al., 2014c), China, Southern Finland (Andronache et al., 2006) and India (Chate et al., 2003). In general, both methods are
       widespread for the estimation of WSCs/BWSCs but few were focused on the differences among these methods.

       In this study, we compare the WSCs/BWSCs estimated from original and updated observational methods with the theoretical
       and model calculations under the same conditions to perform a multimethod evaluation to describe its characteristics. First,
85   we introduce the basic circumstances of the data collected with multiple observation instruments. Then, we present the various
       methods, compare the results and discuss the discrepancies among the different results. Finally, we evaluate the effect of
       below-cloud scavenging on aerosol concentrations and wet depositions based on multimethod techniques.

2 Methods and Data

2.1 Sampling site and measurement data

90   In North China, precipitations were mainly concentrated in summer but rarely in autumn and winter (Xu et al., 2008, Gao et
       al., 2015). However, the air pollution events were usually occurred in autumn and winter in North China Plain (NCP). Here
       we select a typical rainfall event in winter of Beijing (a typical air polluted city in NCP) to study the characteristic of BWSC
       and its implications to aerosol scavenging. The sampling site is situated on top of the two-floor building of the Institute of
       Atmospheric Physics (IAP, 39°58′28″N, 116°22′1″E), located between the north 3rd and 4th Ring Road of Beijing. The site is
95   a typical urban site and is 1 km away from the main road to the north and east, near residential buildings to the south and a
       park to the west, and the pollution at this site is mainly from traffic and domestic sources (Sun et al., 2015). The selected
       rainfall case lasts from 6:56 AM on November 20th to 1:18 AM on November 21st, 2016, which is during the wintertime
       Atmospheric Pollution and Human Health-Beijing (APHH-Beijing) campaign of 2016 (Shi et al., 2018). Thus, comprehensive
       measurements of air pollutants and simulations of pollution mechanisms are available for our use to investigate the wet
100   scavenging process. Fig. s1 shows the radar base reflectivity with echo coverage over the urban area of Beijing from 11:54
       AM on November 20th, and gradually moving from northwest to southeast. The total recorded amount of rainfall is 5.2 mm,
       and the rainfall is more concentrated on the evening of November 20th (beginning at 16:29 PM on November 20th) during this
       event. Notably, the rainfall is nonuniform across Beijing (Song et al., 2015). For example, the recorded rainfall in the southern
       suburban area of Beijing is approximately 7 mm according to the Beijing Meteorological Administration, and this rainfall end
105   at approximately 9:00 AM on November 21st. In this study, the precipitation chemistry and aerosol components sampling
       processes occur at the exact same time at the APHH measurement site.

       An automatic wet-only sequential rainfall sampler is deployed to obtain rainfall samples with 1 mm increments in one
       precipitation event. Four anions (SO_4^{2-}, NO_3^-, Cl^- and F^-) and five cations (NH_4^+, Na^+, K^+, Ca^{2+} and Mg^{2+}) in these samples are
       measured by ion chromatography (IC, Dionex 600, USA). The VWA concentrations of the major soluble inorganic ions, i.e.
110   NO_3^-, SO_4^{2-} and NH_4^+ (hereafter, SNA) in this rainfall are 35.8, 48.7 and 17.5 mg. L^{-1}, respectively, and much higher than the
       VWA concentrations in the winter of 2016 (8.3, 9.5 and 4.1 mg. L^{-1}, respectively) and in previous studies in Beijing (Pan et

al., 2013, 2012;Xu et al., 2017). An ambient ion monitor-ion chromatograph (AIM-IC) developed by URG Corp., Chapel Hill, NC and Dionex Inc., Sunnyvale, CA, is used to measure the $PM_{2.5}$ composition. The time resolution is 60 min. A detailed description of the measured concentration in the rainfall and aerosols can be found in Xu et al. (2017).

115   Thirty meters away from the sampling site, a scanning mobility particle sizer (SMPS) is deployed to observe the particle number size distribution with a 5-min time resolution. The SMPS is used to measure particle number concentration from 14 to 685 nm. A detailed description of the SMPS and methods can be found in Du et al. (2017).

A single-particle aerosol mass spectrometer (SPAMS), which can accurately characterize aerosol particles containing various chemical compositions with diameters ranging from 0.2 to 2.5 μm, is also deployed during the measuring time. More

120   detailed fundamentals of the SPAMS and description can be found in Li et al. (2011), Lin et al. (2017) and Cheng et al. (2018). Size-resolved airborne NO_3^-, SO_4^{2-} and NH_4^+ are the main focuses in this study, and the time resolution is 1 hour. In the meantime, a polarization optical particle counter (POPC) is also deployed to obtain coarse particle (0.4-10.35 μm) size distribution, and time resolution is 5-min. Detailed description and settings can be found in Tian et al. (2018).

2.2 Methods

125   ### 2.2.1 Theoretical basis

Seinfeld and Pandis (1998) proposed the following basic equation of variation of the particle number concentration $N(d_p)$:

$$\frac{dN(d_p)}{dt} = -K(d_p)N(d_p) \tag{1}$$

This equation considers that there is no chemical reaction or emission, and wet scavenging is an exponential process. d_p is the diameter of the aerosol particle, and $K(d_p)$ is the size-resolved BWSC obtained by the following equation:

130   $$K(d_p) = \int_0^\infty \frac{\pi}{4} D_p^2 U_t(D_p) E(D_p, d_p) N(D_p) dD_p \tag{2}$$

where D_p is the raindrop diameter. $U_t(D_p)$ and $N(D_p)$ are the falling terminal velocity and concentration of raindrops, respectively. There are two approaches for describing $U_t(D_p)$: an empirical formula and a physically based formula. Many expressions have been employed for various raindrop diameter ranges. In addition, there are still no available mathematical functions that can accurately characterize the natural raindrop size spectra, and exponential, gamma and lognormal

135   distributions are still used to represent $N(D_p)$ (Wang et al., 2010). Marshall and Palmer (1948) proposed the M-P distribution of raindrop size distribution, which is mostly applied to calculations of BWSCs. $E(D_p, d_p)$ is the collision efficiency of raindrops and aerosol particles, which, in most studies, mainly involves Brownian diffusion, interception and inertial impaction due to dimensional analysis without accounting for thermophoresis, diffusiophoresis and electric charges (Slinn, 1984;Wang et al., 2010). An extensive number of studies have realized that using only the three main mechanisms results in

Atmospheric
Chemistry
and Physics
Discussions

140   underestimation of the collision efficiency, and the contributions from the other mechanisms were added in these studies

(Andronache, 2004c;Andronache et al., 2006;Bae et al., 2010). Assuming that a certain size aerosol particle can be captured

by raindrops of any size, $K(d_p)$ can be calculated theoretically when the falling terminal velocity, raindrop size distribution

and collision efficiency are given. In Wang et al. (2014c)'s study, they added thermophoresis, diffusiophoresis and electric

charges to the quantitative calculation, and we considered this updated to be the theory's result.

2.2.2 Observational method

145

In addition to the theoretical calculation, field observations are also critical for estimating BWSCs. One approach is based on

the change in the number concentration of aerosols (called M1 in this study). When rainfall occurs from t_0 to t_1, Eq (1) can

be integrated as follows:

$$K(d_p) = \frac{1}{t_1 - t_0} \ln[\frac{N_0(d_p)}{N_1(d_p)}]$$ (3)

150   where $N_0(d_p)$ and $N_1(d_p)$ are the measured aerosol particle number concentrations before the rain occurs (t_0) and after

the rain ends (t_1), respectively (Laakso et al., 2003).

In addition, Andronache (2004b) proposed that the WSC can be estimated by the bulk model based on the aerosol mass

balance within a certain bulk, which assumes that there is a box with a horizontal area A and vertical height h above the

observation site. The aerosol flux F on the surface per unit time and area is defined as the following equation:

155    $F = K \times M$ (4)

where K is the WSC and M is the mass of the aerosols in the given box. M can be described as follows:

$M = C_a \times A \times h$ (5)

where C_a is the average aerosol concentration in the box.

In addition, F can also be characterized by the following expression:

160    $F = C_p \times P \times A$ (6)

where C_p is the aerosol concentration in the precipitation collected at the measurement site, P is the precipitation intensity,

and A is the horizontal area for the assumed box. And the wet deposition D_{ep} in a certain time Δt can be expressed as:

$D_{ep} = C_p \times P \times \Delta t = K \times C_a \times h \times \Delta t$ (7)

And K becomes the following expression:

165    $$K = \frac{C_p}{C_a} \times \frac{P}{h}$$ (8)

where C_p and C_a are the paired aerosol concentrations in the precipitation and aerosol, respectively, during rainfall (Okita et al., 1996). In addtion, Andronache (2004b) pointed out that the aerosol concentration in the vertical profile should be considered and updated Eq (8) as follows:

$$K = \frac{C_p}{C_a(0) \times f} \times \frac{P}{h} \qquad (9)$$

170   where $C_a(0)$ is the aerosol concentration at the surface, h is the cloud-base height during rainfall, and

$f = \sum_{z=0}^{z=h} \frac{C_a(z)}{C_a(0)} \times h'(z) / \sum_{z=0}^{z=h} h'(z)$ is the vertical distribution factor of aerosols. Among these variables, $C_a(z)$ are the aerosol

concentrations at the z-level height, respectively, and $h'(z)$ is the depth of the layers in the vertical direction. This approach is called M2.

Moreover, most studies have mentioned that the prevailing wind in Beijing can efficiently reduce the aerosol concentrations

175   (Chan and Yao, 2008; Gonzalez and Aristizabal, 2012). In previous studies by Xu et al. (2017), the north and northwest winds have been recognized as the clear streams to scavenge aerosols in situ, and the effects of clean wind is also considered in this study. In addition, with the help of the 1 mm increments sequential rainfall sampling, Xu et al. (2017) has found that the later increments maintained at a stable, low level, which can be separated into rainout process only. Similar with Eq (9), an updated below-cloud estimated method using $C_{p,below}$ has been developed as Eq (10) and called as M2':

180   $$K = \frac{C_{p,below}}{C_a'(0) \times f} \times \frac{P}{h} \qquad (10)$$

where $C_{p,below}$ is the washout concentration that have been eliminated the rainwater concentrations in each increment and $C_a'(0)$ is the aerosol concentration at the surface that considered the eliminated effects of north and north-west wind.

2.2.3 Modeling calculation

In this study, the Nested Air Quality Prediction Modeling System (NAQPMS) was adopted to calculate the aerosol scavenging

185   coefficient. The RADM-2 mechanism is used for aqueous-phase chemistry, and the subgrid-scale vertical redistribution, dissolution, dissociation and wet deposition are included (Chang et al., 1987). The wet scavenging module used in this study mainly includes below-cloud scavenging process, and the wet scavenging process is briefly described as follows:

$$K = \frac{10.8 \times E \times P^{0.16}}{h} \qquad (11)$$

where E and h are the coagulation kernel and the cloud depth, respectively, and E is usually assumed to be a constant

190   (Wang et al., 2001). In this module, the washout is assumed to be related to precipitation intensity, the aerosol species and so on.

Atmospheric
Chemistry
and Physics
Discussions

To briefly describe these methods, Table 1 lists the formulas. The theoretical estimated scavenging coefficients are labeled Theory. The field observations estimated by Eq (3) and (9) are labeled M1 and M2, respectively. The updated estimated method by Eq (10) is labeled as M2'. The modeling results are labeled M3, and these results are compared with different methods in section 3.

3 Results and Discussion

3.1 Impacts of below-cloud wet scavenging on aerosols

In this case, the total precipitation amount was relatively low, but the precipitation duration was long. SNA represented the majority of the ions in the rainwater, accounting for 73% of the total and their temporal variations are shown in Fig. 1. The precipitation duration is marked with the blue frame. In the early stage, marked with light blue stripes, the precipitation duration was long and the precipitation intensity was weak. In the later period, from 16:29 PM on November 20th to 1:18 AM on November 21st, the precipitation began to strengthen and is marked with the blue shading. Before this event, a severe haze occurred which exceeded the National Ambient Air Quality Standard (NAQQS, 75 µg.m^{-3}) (Shi et al., 2018). When rain occurred, both the aerosols in the air and the SNA concentration in the rainwater gradually decreased, especially during the later stage. It's clearly visible in Fig. 1 that all aerosol concentrations on the rainy day were much lower than the hourly average aerosol concentrations during the APHH campaign. Following the rain, SNA reached relatively stable and low values. For example, SO_4^{2-} decreased from 70.6 to 25.2 mg. L[-1] (or a reduction of 64.3%) in the rainwater. Accordingly, aerosol sulfate and decreased by nearly 6 µg.m^{-3} in the air.

The time series and averaged spectrum distribution of particle number size distributions measured by POPC, SPAMS and SMPS are shown in Fig. 2. With the help of three instruments, the size distributions cover a rather wide range, from 0.014 to 10.35 µm. The spectrum distribution exhibited unimodal distributions peaked in the size range of 20-90 nm. The spectrum distribution for SPAMS of NO_3^- and SO_4^{2-} both showed particularly high consistency in terms of variation patterns, magnitude and particle size distribution (Lang et al., 2016). And for POPC, the trend was also in consistent well with the coarse size of SPAMS. As shown from Fig. 2(a), for POPC and SMPS, the number concentration did not immediately decrease due to relatively weak precipitation intensity before 16:29 PM on November 20th. And in the later period, the number concentration decreased sharply and remained at a low level. It agreed well with the radar echo and precipitation intensity during this rain event. In order to investigate the BWSC, 16:29 PM on November 20th is taken as the before the rain occurs time in calculating the M1 and it will not repeat in following sections.

3.2 Multimethod comparison of BWSCs

For further analysis, the estimated BWSCs based on multiple methods were compared and shown in Fig. 3. As for the observational methods, e.g., M1, M2 and M2', there is no significant difference in the range of magnitude between them. More specifically, the observed BWSCs by original M2 are larger than the updated M2' method. However, M2' ($5.7×10^{-5}$, $8.9×10^{-5}$

Atmospheric
Chemistry
and Physics
Discussions

and 5.4×10^{-5} s^{-1} for NO$_3^-$, SO$_4^{2-}$ and NH$_4^+$) is much closer to the results of M1 (~10^{-5} s^{-1} for particle size in the range of 0.014-10.35 μm). Since M1 is based on the variations of the aerosol numbers below the cloud, it may be more suitable for the

225 estimation of the BWSCs. It also indicates that the updated M2' is much more reasonable than the original M2 for estimation of BWSCs of various chemical species. In contrast, the theory calculated BWSC as 1.9×10^{-6} s^{-1} has an order of magnitude lower than the observational results. Considering the effects of thermophoresis, diffusiophoresis and electric charges, there is a wider range of three orders of magnitude (10^{-6}-10^{-4} s^{-1}) (Wang et al., 2010;Wang et al., 2014c). In addition, the BWSC for M3 (3.2×10^{-6} s^{-1}) is also one order of magnitude lower than the field measurements. The low BWSC in CTMs can explain the

230 underestimation of simulated wet deposition, which is mainly thought caused by chemical process, modeled precipitation and emission in previous studies (Wang et al., 2008;Ge et al., 2011). Thus, the observed M1 and M2' may revise the theory and M3 results in the future.

To further compare the BWSCs based on the particle size, the results in this study are compared with those of previous studies in Fig. 4. The size-resolved BWSCs of 0.014-0.74, 0.2-2.5 and 0.7-10.35 μm are the total number concentration by

235 SMPS, SPAMS and POPC, respectively, which are within a certain range (1.81×10^{-5}-8.53×10^{-5} s^{-1}). At approximately 0.2 μm (the lower limit detection of the multicomponent analysis), the M1 of 0.014-0.74 and 0.2-2.5 μm results have a gap that mainly originates from the use of different experimental instruments and their detection limits. However, the estimated results for larger sizes ($d_p > 3$ μm) by POPC have great fluctuation, mainly due to less number concentrations (< 2 cm^{-3}) and were considered as unreliable in this work. The BWSC from M1 showed a slowly decreasing trend in 0.014-0.2 μm and a significant

240 increasing trend as $d_p > 0.2$ μm in this study, which is similar with the results of Huang Mountain (Wang et al., 2014c) and southern Finland (Laakso et al., 2003). Besides, the BWSC from M2' for SNA are similar to the results of M1 in 2.5 μm. Although there is a different trend with that reported in Lanzhou (Zhao et al., 2015) before 0.6 μm, both study exhibited an increasing trend after 0.6 μm. The difference of BWSCs from M1 in each sites may due to the measuring conditions (Wang et al., 2010). However, compared to the theory methods, this difference is very small as shown in Fig. 5. Different from the

245 observational results, the theoretical results show a strong dependence on the particle size with obvious decreasing trend ($d_p < 1$ μm) and quickly increasing trend ($d_p > 1$ μm). As Seinfeld and Pandis (1998) mentioned, Brownian diffusion and gravity are the principal mechanisms affecting collection efficiency with d_p smaller than 0.2 μm and larger than 2.5 μm, respectively. Theoretical estimation can effectively characterize the observed BWSC of aerosols in these two ranges. For the "Greenfield gap", there is large difference between the BWSC from M1 and theory method with the later is one order of magnitude lower.

250 One reason is that all the influencing mechanisms still have not been fully considered and understood (Seinfeld, 1998), another reason is the existing ideal assumptions in derivation, such as no chemical reactions or emissions in the scavenging process; Ignored irregular surface of the aerosols and hygroscopic growth will increase the concentration of particles and then influence the scavenging efficiency (Wang et al., 2014c). Other extensive explanation is that the turbulent flow fluctuation, evaporation and breakup of raindrops are also important but neglected processes (Wang et al., 2010).

3.3 The parameterization of BWSCs

To discuss the uncertainties of the BWSC underestimation by theoretical calculations in different rainfall events, the data in summer of 2014 have also been included. As shown in Fig. 5, a strong relationship between the BWSCs and precipitation intensity obeys exponential power distribution both in summer of 2014 and the rainfall event in winter of APHH campaign in Beijing with the correlation coefficients for SNA are over than 0.68. Since the estimated BWSCs for SNA based on M1 and M2' in this event are in line with previous studies in summer, it indicated that the wet scavenging rule and regression fitting formulas are also universal in Beijing not only in summer but also in winter. In fact, this exponential power relationship has been confirmed in previous studies (Jylhä, 1991;Okita et al., 1996;Andronache, 2004a;Wang et al., 2014a;Wang et al., 2014b;Xu et al., 2017):

$$K = a \times P^b \tag{12}$$

where parameter b represents the change rate of BWSCs along with P, while a is equal to the WSCs when the $P = 1$ mm/h. Both a and b relate to chemical species and aerosols particle size.

For the further comparison, Fig.6 displays the parameterization of a and b in the exponential power relationship for BWSCs with the precipitation intensity by multimethod, i.e., theoretical method and field measurement methods. For the theory calculation, the parameter a varies from a relatively wide range of 2.8×10^{-8}-6.7×10^{-5} s^{-1} and BWSCs also have a wide range of 3-4 orders of magnitude for given precipitation intensities (Andronache, 2003;Wang et al., 2014b). Similar with the multimethod comparison of estimated BWSCs in this rainfall event of APHH campaign, parameterization for BWSCs obtained by M2/M2' shows higher magnitude of variations with the precipitation intensity with all of the straight line lie above the upper range of the theory calculation. It indicates recent theory calculated BWSCs has an obvious underestimation not only in a rainfall event but also in the parameterization of large number of rainfall events with different precipitation intensities and need revised or updated by the field measurement estimation.

3.4 Impacts and implications

To investigate the impacts of the wet scavenging on aerosol concentrations in the air and the wet depositions in rainfall, multimethod-estimated BWSCs included in Table 2 were used to rebuild the aerosol concentrations and wet depositions after one hour of rainfall event. Assuming the aerosol concentrations in the air are only influenced by the wet scavenging during rainfall event, its variation should be followed by Eq (13) according to Seinfeld and Pandis (1998):

$$\frac{dC_a}{dt} = -KC_a \tag{13}$$

$$C_a = C_{a0} e^{-Kt} \tag{14}$$

Variations of aerosol concentration can be resolved as Eq (14), in which the K is a constant BWSC. Where, K and t are the BWSCs and the scavenging time, and C_{a0} is the original aerosol concentration before the rainfall. In this study, the

285   C_{a0} have been observed as 17.6 µg.m^{-3}, 9.8 µg.m^{-3}, 9.7 µg.m^{-3} and 74.7 µg.m^{-3} for NO$_3^-$, SO$_4^{2-}$, NH$_4^+$ and PM$_{2.5}$, respectively. After one hour of the wet scavenging by rainfall, the concentration of NO$_3^-$, SO$_4^{2-}$, NH$_4^+$ and PM$_{2.5}$ decreased to 14.3 µg.m^{-3}, 7.6 µg.m^{-3}, 7.9 µg.m^{-3} and 65.2 µg.m^{-3} respectively. Previous studies have confirmed that the exponential power distribution between the WSCs and precipitation intensity as Eq (12). And the size-resolved BWSC are accumulated for calculating the total BWSC for PM$_{2.5}$. As it is shown in Table 2, except CAMx, the calculated aerosol concentrations using theory and M3

290 BWSCs performed the obvious overestimation of PM$_{2.5}$ concentrations with the bias from 2.3 µg.m^{-3} to 9 µg.m^{-3}, while showed similar with the observation for M1 and M2' BWSCs (bias < 1 µg.m^{-3}). It should be noted that the magnitude of BWSCs in the range of 10^{-5}-10^{-4} perform the better-calculated aerosol concentrations than that the lower range. Wet deposition has also been reconstructed according to Eq (7), with the precipitation intensity setting as 0.17 mm/h, and the column height considering as 3 km. The Net Mean Bias (NMB) for the below-cloud wet depositions of NO$_3^-$ and NH$_4^+$ are -28% and -33%, while for SO$_4^{2-}$

295 is -49% according to the BWSCs in this study shown in Table 2.

    Overall, the M1 and updated M2' field observation results can effectively characterize the below-cloud scavenging ability whereas theory and M3 have obvious deviation. Therefore, the field measurements are needed to compensate for the defects in the theoretical and modeling calculations that provides room to make further progress in wet deposition numerical simulation.

4 Conclusions

300 An evaluation of below-cloud wet scavenging ability is first conducted based on field measurements, and accompanied with the theoretical estimation and modeling calculation. The averaged BWSCs obtained by field measurements are similar to each other of 10^{-5} s^{-1} and there exists strong exponential power relationship between BWSCs and precipitation intensity. Theoretical estimations coincide well with the observed BWSCs of aerosols with the d_p in ranges of smaller than 0.2 µm and larger than 2.5 µm, but are one magnitude lower than observed BWSCs within 0.2-2.5 µm. In the form of exponential power distribution

305 of BWSCs with precipitation intensity, the upper range of theoretical results is also lower than the measurement estimation. Thus, the underestimation of BWSC through theoretical method has been confirmed not only in APHH-Beijing campaign but also in all rainfall events in summer of 2014. These theoretical values are usually applied in CTMs with simplified scheme and accordingly the model calculations show lower BWSCs. It may explain the underprediction of the wet deposition both in global and in regional models of polluted regions. Field measurements are currently required to compensate for the theoretical

310 and modeling calculations and to construct a more reasonable and suitable simulation scheme to improve the wet deposition simulation, especially in polluted regions.

Competing interests

The authors declare that they have no conflict of interest.

Atmospheric
Chemistry
and Physics
Discussions

Open Access

EGU

Author contribution

315 DX, BG and ZW designed the whole structure of this work, XC performed the modeling calculation, YS, NC, ML, XP, ZM and YP prepared the SMPS data, the POPC data and the SPAMS data, respectively. DX performed the sequential sampling of rainwater, analyzed the data. DX and BG prepared the manuscript with contributions from all-authors.

Acknowledgment

Reference :

Andronache, C.: Estimated variability of below-cloud aerosol removal by rainfall for observed aerosol size distributions, Atmos Chem Phys, 3, 131-143, 2003.

325 Andronache, C.: Precipitation removal of ultrafine aerosol particles from the atmospheric boundary layer, J Geophys Res-Atmos, 109, 2004a.

Andronache, C.: Estimates of sulfate aerosol wet scavenging coefficient for locations in the Eastern United States, Atmos Environ, 38, 795-804, http://dx.doi.org/10.1016/j.atmosenv.2003.10.035, 2004b.

Andronache, C.: Diffusion and electric charge contributions to below-cloud wet removal of atmospheric ultra-fine aerosol

330 particles, J Aerosol Sci, 35, 1467-1482, 2004c.

Andronache, C., nholm, T. G., Laakso, L., Phillips, V., and inen, A. V. l.: Scavenging of ultrafine particles by rainfall at a boreal site: observations and model estimations, Atmospheric Chemistry and Physics (ACP) & Discussions (ACPD), 2006.

Bae, S. Y., Jung, C. H., and Kim, Y. P.: Derivation and verification of an aerosol dynamics expression for the below-cloud scavenging process using the moment method, J Aerosol Sci, 41, 266-280, https://doi.org/10.1016/j.jaerosci.2009.11.006,

335 2010.

Barth, M. C., Rasch, P. J., Kiehl, J. T., Benkovitz, C. M., and Schwartz, S. E.: Sulfur chemistry in the National Center for Atmospheric Research Community Climate Model: Description, evaluation, features, and sensitivity to aqueous chemistry, Journal of Geophysical Research: Atmospheres, 105, 1387-1415, 10.1029/1999jd900773, 2000.

Chan, C. K., and Yao, X.: Air pollution in mega cities in China, Atmos Environ, 42, 1-42, 10.1016/j.atmosenv.2007.09.003,

340 2008.

Chang, J. S., Brost, R. A., Isaksen, I. S. A., Madronich, S., Middleton, P., Stockwell, W. R., and Walcek, C. J.: A 3-Dimensional Eulerian Acid Deposition Model - Physical Concepts and Formulation, J Geophys Res-Atmos, 92, 14681-14700, Doi 10.1029/Jd092id12p14681, 1987.

Chate, D. M., Rao, P. S. P., Naik, M. S., Momin, G. A., Safai, P. D., and Ali, K.: Scavenging of aerosols and their chemical

345 species by rain, Atmos Environ, 37, 2477-2484, http://dx.doi.org/10.1016/S1352-2310(03)00162-6, 2003.

Chatterjee, A., Jayaraman, A., Rao, T. N., and Raha, S.: In-cloud and below-cloud scavenging of aerosol ionic species over a tropical rural atmosphere in India, J Atmos Chem, 66, 27-40, 10.1007/s10874-011-9190-5, 2010.

Cheng, C., Huang, Z., Chan, C. K., Chu, Y., Li, M., Zhang, T., Ou, Y., Chen, D., Cheng, P., Li, L., Gao, W., Huang, Z., Huang, B., Fu, Z., and Zhou, Z.: Characteristics and mixing state of amine-containing particles at a rural site in the Pearl River

350 Delta, China, Atmos. Chem. Phys., 18, 9147-9159, 10.5194/acp-18-9147-2018, 2018.

Du, W., Zhao, J., Wang, Y., Zhang, Y., Wang, Q., Xu, W., Chen, C., Han, T., Zhang, F., Li, Z., Fu, P., Li, J., Wang, Z., and Sun, Y.: Simultaneous measurements of particle number size distributions at ground level and 260 m on a meteorological tower in urban Beijing, China, Atmos. Chem. Phys., 17, 6797-6811, 2017.

Gao, X. D., Chen, X Y., Ding, Z. W., Yang, W. Q. 2015. Investigation of the variation of atmospheric pollutants from chemical
composition of precipitation along an urban-to-rural transect in Beijing. Acta Scientiae Circumstantiae (in Chinese),
35(12): 4033-4042.

Ge, B Z., Wang, Z F., Gbaguidi, A. E., and Zhang, Q.: Source Identification of Acid Rain Arising over Northeast China:
Observed Evidence and Model Simulation, Aerosol Air Qual Res, 16, 1366-1377, 10.4209/aaqr.2015.05.0294, 2016.

Ge, B. Z., Wang, Z. F., Xu, X. B., Tang, J., He, Y. J., Uno, I., and Ohara, T.: Impact of the East Asian summer monsoon on
long-term variations in the acidity of summer precipitation in Central China, Atmos Chem Phys, 11, 1671-1684, DOI
10.5194/acp-11-1671-2011, 2011.

Gonzalez, C. M., and Aristizabal, B. H.: Acid rain and particulate matter dynamics in a mid-sized Andean city: The effect of
rain intensity on ion scavenging, Atmos Environ, 60, 164-171, 2012.

Jylhä, K.: Empirical scavenging coefficients of radioactive substances released from Chernobyl, 1991.

Laakso, L., Grönholm, T., Rannik, Ü., Kosmale, M., Fiedler, V., Vehkamäki, H., and Kulmala, M.: Ultrafine particle scavenging
coefficients calculated from 6 years field measurements, Atmos Environ, 37, 3605-3613, https://doi.org/10.1016/S1352-
2310(03)00326-1, 2003.

Liu, L.; Zhang, W. J.; D, S. Y.; Hou, L. J.; Han, B.; Yang, W.; Chen, M. D.; Bai, Z. P.,: Seasonal Variation Characteristics and
Potential Source Contribution of Sulfate, Nitrate and Ammonium in Beijing by Using Single Particle Aerosol Mass
Spectrometry, Environmental Science (in Chinese), 37, 1609-1618, 2016.

Li, L., Huang, Z., Dong, J., Li, M., Gao, W., Nian, H., Fu, Z., Zhang, G., Bi, X., Cheng, P., and Zhou, Z.: Real time bipolar
time-of-flight mass spectrometer for analyzing single aerosol particles, International Journal of Mass Spectrometry, 303,
118-124, https://doi.org/10.1016/j.ijms.2011.01.017, 2011.

Lin, Q., Zhang, G., Peng, L., Bi, X., Wang, X., Brechtel, F. J., Li, M., Chen, D., Peng, P., Sheng, G., and Zhou, Z.: In situ
chemical composition measurement of individual cloud residue particles at a mountain site, southern China, Atmos. Chem.
Phys., 17, 8473-8488, 10.5194/acp-17-8473-2017, 2017.

Luo, G., Yu, F. Q., and Schwab, J.: Revised treatment of wet scavenging processes dramatically improves GEOS-Chem 12.0.0
simulations of nitric acid, nitrate, and ammonium over the United States, Geosci. Model Dev. Discuss., 2019, 1-18,
10.5194/gmd-2019-58, 2019.

Marshall, J. S., and Palmer, W. M.: The distribution of raindrop with size, Journal of Meteorology and Environment, 5, 165-
166, 1948.

Hu, M., Jing, Z., and Wu, Z. J.: Chemical compositions of precipitation and scavenging of particles in Beijing, Sci China Ser
B, 48, 265-272, 10.1360/042004-49, 2005.

Okita, T., Hara, H., and Fukuzaki, N.: Measurements of atmospheric SO2 and SO42-, and determination of the wet scavenging
coefficient of sulfate aerosols for the winter monsoon season over the Sea of Japan, Atmos Environ, 30, 3733-3739, 1996.

Pan, Y. P., Wang, Y. S., Tang, G. Q., and Wu, D.: Wet and dry deposition of atmospheric nitrogen at ten sites in Northern China,
Atmos Chem Phys, 12, 6515-6535, 2012.

Pan, Y. P., Wang, Y. S., Tang, G. Q., and Wu, D.: Spatial distribution and temporal variations of atmospheric sulfur deposition in Northern China: insights into the potential acidification risks, Atmos Chem Phys, 13, 1675-1688, 2013.

390 Seinfeld, J. H., and S.N. Pandis. 1998. ,: From Air Pollution to Climate Change. John Wiley and Sons, Inc., NY., Atmospheric Chemistry and Physics, 1998.

Shi, Z. B.; Vu, T.; Kotthaus, S.; Grimmond, S.; Harrison, R. M.; Yue, S. Y.; Zhu, T.; Lee, J.; Han, Y. Q.; Demuzere, M.; Dunmore, R. E.; Ren, L. J.; Liu, D.; Wang, Y. L.; Wild, O.; Allan, J.; Barlow, J.; Beddows, D.; Bloss, W. J.; Carruthers, D.; Carslaw, D. C.; Chatzidiakou, L.; Crilley, L.; Coe, H.; Dai, T.; Doherty, R.; Duan, F. K.; Fu, P. Q.; Ge, B. Z.; Ge, M.
395 F.; Guan, D. B.; Hamilton, J. F.; He, K. B.; Heal, M.; Heard, D.; Hewitt, C. N.; Hu, M.; Ji, D. S.; Jiang, X. J.; Jones, R.; Kalberer, M.; Kelly, F. J.; Kramer, L.; Langford, B.; Lin, C.; Lewis, A. C.; Li, J.; Li, W. J.; Liu, H.; Loh, M.; Lu, K. D.; Mann, G.; McFiggans, G.; Miller, M.; Mills, G.; Monk, P.; Nemitz, E.; O'Connor, F.; Ouyang, B.; Palmer, P. I.; Percival, C.; Popoola, O.; Reeves, C.; Rickard, A. R.; Shao, L. Y.; Shi, G. Y.; Spracklen, D.; Stevenson, D.; Sun, Y. L.; Sun, Z. W.; Tao, S.; Tong, S. R.; Wang, Q. Q.; Wang, W. H.; Wang, X. M.; Wang, Z. F.; Whalley, L.; Wu, X. F; Wu, Z. J.; Xie, P. H.;
400 Yang, F. M; Zhang, Q.; Zhang, Y. L.; Zhang, Y. H.; Zheng, M.: Introduction to Special Issue-In-depth study of air pollution sources and processes within Beijing and its surrounding region (APHH-Beijing), Atmos. Chem. Phys. Discuss., 2018, 1-62, 10.5194/acp-2018-922, 2018.

Slinn, W. G. N.: Precipitation scavenging, in: Atmospheric Science and Power Production, edited by: Randerson, D., Doc. DOE/TIC-27601, Tech. Inf. Cent., Off. Of Sci. and Tech. Inf., U.S. Dep. Of Energy, Washington, D.C, 1984.

405 Song, X., Zhang, J., Aghakouchak, A., Roy, S. S., Xuan, Y., Wang, G., He, R., Wang, X., and Liu, C.: Rapid urbanization and changes in spatiotemporal characteristics of precipitation in Beijing metropolitan area: PRECIPITATION VARIATION IN BEIJING, Journal of Geophysical Research Atmospheres, 119, 11,250-211,271, 2015.

Stier, P., Feichter, J., Kinne, S., Kloster, S., Vignati, E., Wilson, J., Ganzeveld, L., Tegen, I., Werner, M., Balkanski, Y., Schulz, M., Boucher, O., Minikin, A., and Petzold, A.: The aerosol-climate model ECHAM5-HAM, Atmos. Chem. Phys., 5, 1125-
410 1156, 10.5194/acp-5-1125-2005, 2005.

Sun, Y. L., Wang, Z. F., Du, W., Zhang, Q., Wang, Q. Q., Fu, P. Q., Pan, X. L., Li, J., Jayne, J., and Worsnop, D. R.: Long-term real-time measurements of aerosol particle composition in Beijing, China: seasonal variations, meteorological effects, and source analysis, Atmos Chem Phys, 15, 10149-10165, 10.5194/acp-15-10149-2015, 2015.

Tang, X. Y., Zhang, Y. H., and Shao, M.: Atmospheric environment and chemical, Beijing: Higher education press, 2006.

415 Textor, C., Schulz, M., Guibert, S., Kinne, S., Balkanski, Y., Bauer, S., Berntsen, T., Berglen, T., Boucher, O., Chin, M., Dentener, F., Diehl, T., Easter, R., Feichter, H., Fillmore, D., Ghan, S., Ginoux, P., Gong, S., Kristjansson, J. E., Krol, M., Lauer, A., Lamarque, J. F., Liu, X., Montanaro, V., Myhre, G., Penner, J., Pitari, G., Reddy, S., Seland, O., Stier, P., Takemura, T., and Tie, X.: Analysis and quantification of the diversities of aerosol life cycles within AeroCom, Atmos Chem Phys, 6, 1777-1813, 2006.

420 Tian, Y., Pan, X. L., Nishizawa, T., Kobayashi, H., Uno, I., Wang, X., Shimizu, A., and Wang, Z. F.: Variability of depolarization of aerosol particles in the megacity of Beijing: implications for the interaction between anthropogenic pollutants and

mineral dust particles, Atmos. Chem. Phys., 18, 18203-18217, 10.5194/acp-18-18203-2018, 2018.

Vet, R., Artz, R. S., Carou, S., Shaw, M., Ro, C. U., Aas, W., Baker, A., Bowersox, V. C., Dentener, F., Galy-Lacaux, C., Hou, A., Pienaar, J. J., Gillett, R., Forti, M. C., Gromov, S., Hara, H., Khodzher, T., Mahowald, N. M., Nickovic, S., Rao, P. S.
425   P., and Reid, N. W.: A global assessment of precipitation chemistry and deposition of sulfur, nitrogen, sea salt, base cations, organic acids, acidity and pH, and phosphorus, Atmos Environ, 93, 3-100, 2014.

Wang, X. H.; Zhang, L. M.; Moran, M. D.,: Uncertainty assessment of current size-resolved parameterizations for below-cloud particle scavenging by rain, Atmos. Chem. Phys., 10, 5685-5705, 10.5194/acp-10-5685-2010, 2010.

Wang, X. H.; Zhang, L. M.; Moran, M. D.,: Bulk or modal parameterizations for below-cloud scavenging of fine, coarse, and
430   giant particles by both rain and snow, Journal of Advances in Modeling Earth Systems, 6, 1301-1310, 10.1002/2014ms000392, 2014a.

Wang, X. H.; Zhang, L. M.; Moran, M. D.,: Development of a new semi-empirical parameterization for below-cloud scavenging of size-resolved aerosol particles by both rain and snow, Geosci Model Dev, 7, 799-819, 10.5194/gmd-7-799-2014, 2014b.

435   Wang, Y., Zhu, B., Kang, H. Q, Gao, J. H., Jiang, Q., and Liu, X. H.: Theoretical and observational study on below-cloud rain scavenging of aerosol particles, Journal of University of Chinese Academy of Sciences (in Chinese), 31, 306-321, 2014c.

Wang, Z., Maeda, T., Hayashi, M., Hsiao, L. F., and Liu, K. Y.: A nested air quality prediction modeling system for urban and regional scales: Application for high-ozone episode in Taiwan, Water Air Soil Poll, 130, 391-396, 2001.

Wang, Z. F., Xie, F. Y., Sakurai, T., Ueda, H., Han, Z. W., Carmichael, G. R., Streets, D., Engardt, M., Holloway, T., Hayami,
440   H., Kajino, M., Thongboonchoo, N., Bennet, C., Park, S. U., Fung, C., Chang, A., Sartelet, K., and Amann, M.: MICS-Asia II: Model inter-comparison and evaluation of acid deposition, Atmos Environ, 42, 3528-3542, 2008.

Xu, D. H., Ge, B. Z., Wang, Z. F., Sun, Y. L., Chen, Y., Ji, D. S., Yang, T., Ma, Z. Q., Cheng, N. L., Hao, J. Q., and Yao, X. F.: Below-cloud wet scavenging of soluble inorganic ions by rain in Beijing during the summer of 2014, Environ Pollut, 230, 963-973, https://doi.org/10.1016/j.envpol.2017.07.033, 2017.

445   Xu, J., Zhang, X. L., Xu, X. B., Ding, G. A., Yan. P., Yu, X. L., Chen, H. B., Zhou, H. G. 2008. Variations and source identification of chemical compositions in wet deposition at Shangdianzi background station. Acta Scientiae Circumstantiae (in Chinese), 28(5):1001 -1006.

Yamagata, S., Kobayashi, D., Ohta, S., Murao, N., Shiobara, M., Wada, M., Yabuki, M., Konishi, H., and Yamanouchi, T.: Properties of aerosols and their wet deposition in the arctic spring during ASTAR2004 at Ny-Alesund, Svalbard, Atmos
450   Chem Phys, 9, 261-270, 2009.

Zhang, L., Michelangeli, D. V., and Taylor, P. A.: Numerical studies of aerosol scavenging by low-level, warm stratiform clouds and precipitation, Atmos Environ, 38, 4653-4665, https://doi.org/10.1016/j.atmosenv.2004.05.042, 2004.

Zhao, S., Yu, Y., He, J., Yin, D., and Wang, B.: Below-cloud scavenging of aerosol particles by precipitation in a typical valley city, northwestern China, Atmos Environ, 102, 70-78, https://doi.org/10.1016/j.atmosenv.2014.11.051, 2015.

455   Zhu, J., Tang, X., Wang, Z. F., and Wu, L.: A Review of Air Quality Data Assimilation Methods and Their Application, Journal

of Atmospheric Sciences (in Chinese), 42, 607-620, 2018.

Table 1. List of multimethod calculations for the BWSCs

	Formula	Reference	Symbol
Theory	$K(d_p) = \int_0^\infty \frac{\pi}{4} D_p^2 U_t(D_p) E(D_p, d_p) N(D_p) dD_p$	Seinfeld and Pandis (1998), Wang et al. (2014c)	Theory
Field Observation	$K(d_p) = \frac{1}{t_1 - t_0} \ln[\frac{N_0(d_p)}{N_1(d_p)}]$	Laakso et al. (2003)	M1
	$K = \frac{C_p}{C_a(0) \times f} \times \frac{P}{h}$	Andronache (2004b)	M2
	$K = \frac{C_{p,below}}{C_a'(0) \times f} \times \frac{P}{h}$	Xu et al. (2017)	M2'
Modeling calculation	$K = \frac{10.8 \times E \times P^{0.16}}{h}$	Wang et al. (2001)	M3

460

Table 2. The observed aerosol concentration and wet deposition, and parameters of the exponential power fittings, WSCs, rebuilt aerosol concentrations and wet depositions after one hour compare with multimethod.

Source	Species	$K = aP^b$		BWSC (s^{-1})	Aerosol concentration $(\mu g.m^{-3})$	Wet deposition $(mg.m^{-2})$	Supplementary information
		a	b				
	NO_3^-				14.3	3.2	
	SO_4^{2-}				7.6	5.9	Observed aerosol concentrations and wet depositions after one-hour rainfall
	NH_4^+				7.9	1.8	
	$PM_{2.5}$				65.2	-	
	NO_3^-	2.5×10^{-4}	0.61	5.7×10^{-5}	14.4	2.3	
This study [a]	SO_4^{2-}	7.6×10^{-5}	0.80	8.9×10^{-5}	7.1	3.0	Winter in Beijing, M2'
	NH_4^+	1.1×10^{-4}	0.52	5.4×10^{-5}	8.0	1.2	
This study [a]	PM	-	-	4.1×10^{-5}	64.6	-	0.014-10.35 μm, winter in Beijing, M1
Okita et al. (1996) [a*]	SO_4^{2-}	1.38×10^{-4}	0.74	3.8×10^{-5}	8.6	0.6	Sado, Japan, winter of 1992, M2
Andronache (2004b) [a*]	SO_4^{2-}	4.0×10^{-4}	0.81	9.5×10^{-4}	7.0	3.3	AIRMoN in the USA, M2
Yamagata et al. (2009) [a*]	SO_4^{2-}	-	-	9.8×10^{-6}-2.5×10^{-4}	4.0-9.5	0.04-15.8	The Arctic, late spring of 2004, M2
Laakso et al. (2003) [a]	PM	-	-	9.1×10^{-6}	72.3	-	0.01-0.51 μm, southern Finland, 6 years of observations, M1
Wang et al. (2014c) [a]	PM	4.2×10^{-5}	0.16	3.1×10^{-5}	66.7	-	0.01-1 μm, Huang Mountain, 2001 summer, M1
Zhao et al. (2015) [a]	PM	-	-	3.2×10^{-5}	66.6	-	0.01-10 μm, Lanzhou, 2012.9-2013.8, M1
This study [b]	$PM_{2.5}$			1.9×10^{-6}	74.2	-	Theory

Wang et al. (2014b) [b]	PM$_{2.5}$	3.83×10^{-7}-6.89×10^{-4}	0.64-0.91	10^{-8}-10^{-2}	-	-
This study [c]	PM$_{2.5}$	-	-	3.2×10^{-6}	73.8	-	NAQPMS, M3
Luo et al. (2019) [c]	PM$_{2.5}$	-	-	2.8×10^{-5}	67.5	-	GEOS-Chem
ENVIRON.Inc (2005) [c]	PM$_{2.5}$	4.2×10^{-4}	0.79	1.8×10^{-4}	51.3	-	CAMx

[a] field observation, [b] theory and [c] modeling calculation

[*] WSC and [**] the wet scavenging effects on PM$_{2.5}$

Figure captions

Figure 1. Hourly average aerosol concentration during November 11th to December 11th (box) and the rainy period on November 20th to 21st (red line and hollow circles) for (a) NO_3^-, (b) SO_4^{2-} and (c) NH_4^+. The rainwater concentrations are shown as follows: (a) NO_3^-, blue; (b) SO_4^{2-}, red; and (c) NH_4^+, orange (line and triangles). Time series of the NO_3^- (blue), SO_4^{2-} (red) and NH_4^+ (orange) concentrations in the rainfall (lines and triangles) and in the air (lines) (d).

Figure 2. Time series of particle number size distributions (a) are measured by POPC, SPAMS (take SO_4^{2-} for example) and SMPS, respectively. The averaged spectrum distribution of number concentration during the APHH-Beijing campaign (a) for SMPS (purple line), POPC (green line) and NO_3^- (blue line), SO_4^{2-} (red line) and NH_4^+ (orange line) by SPAMS.
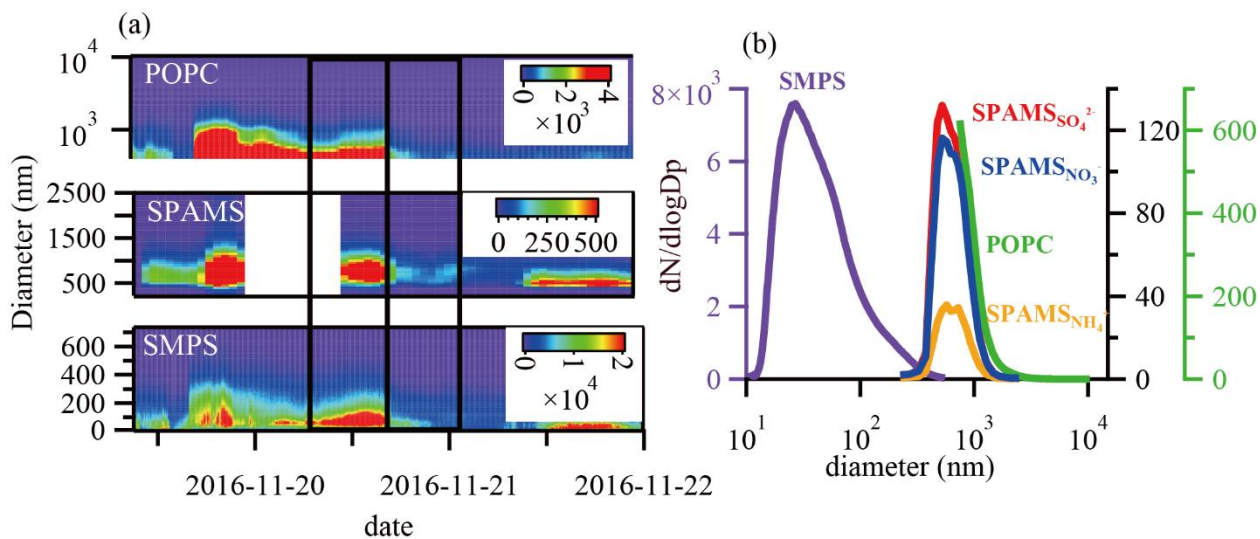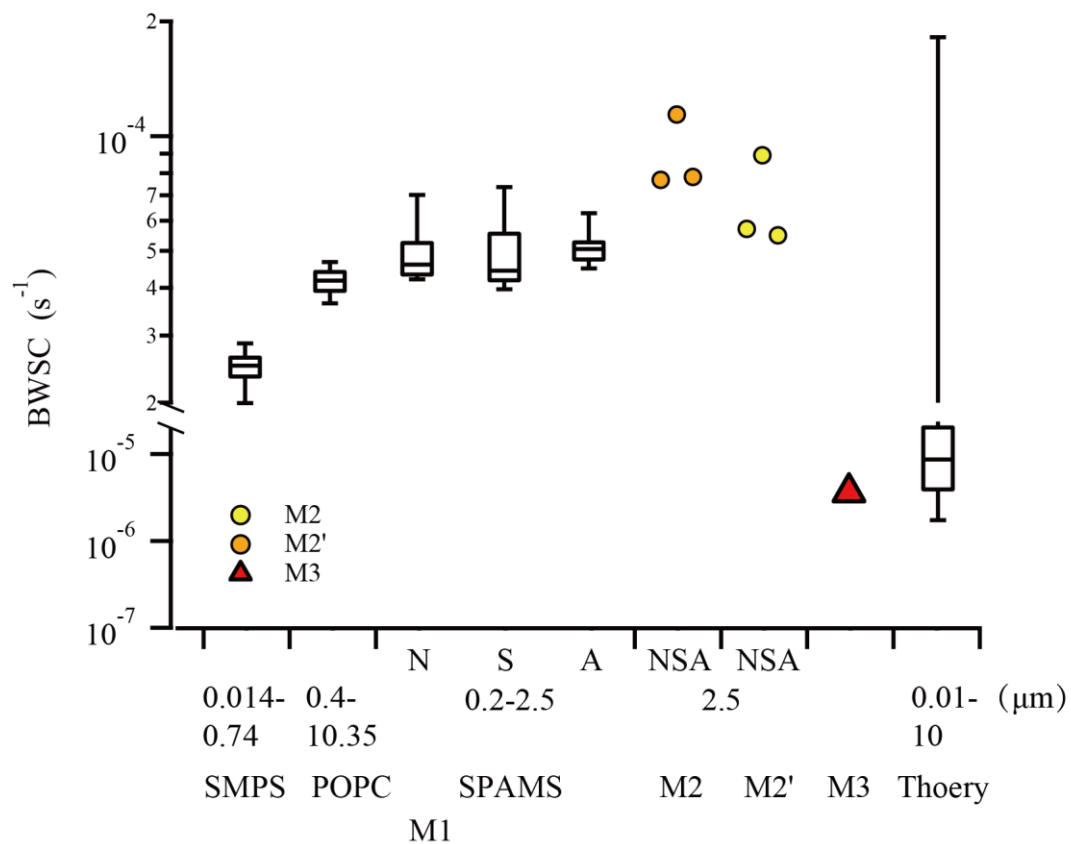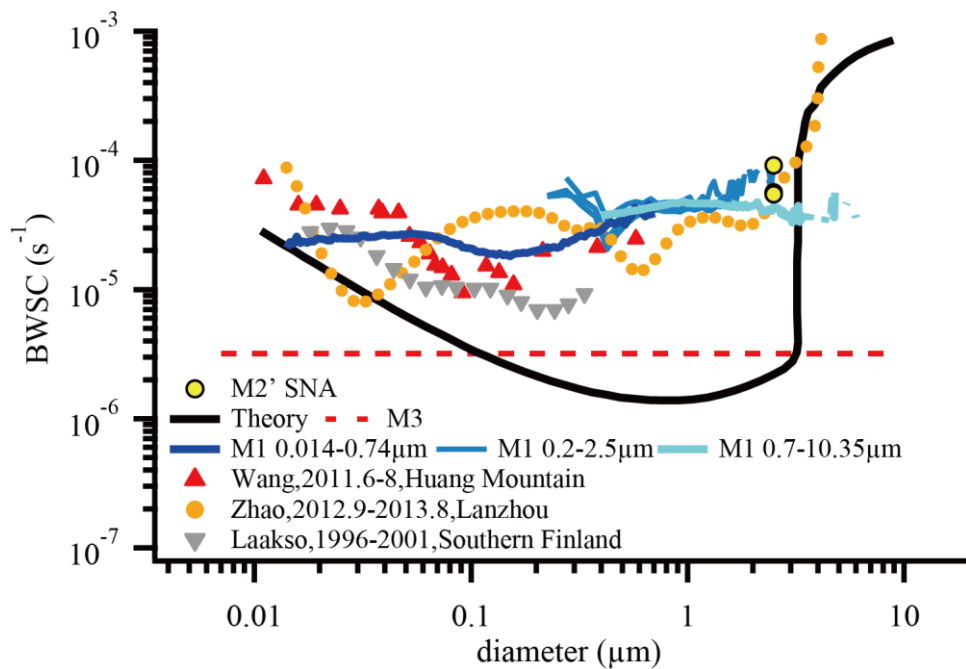
Figure 3. Multimethod estimation of the BWSCs.

Figure 4. Multimethod estimation of the BWSCs and comparisons with previous studies.

Figure 5. Scatter plots of the BWSCs and precipitation intensity for NO_3^- (a), SO_4^{2-} (b) and NH_4^+ (c) (black dots: M2' in summer by Xu et al. (2017), light blue triangle: M2' in this case, deep blue triangle: M1).

Figure 6. The parameterization of BWSCs with the rainfall intensities.

Figure 1. Hourly average aerosol concentration during November 11th to December 11th (box) and the rainy period on November 20th to 21st (red line and hollow circles) for (a) NO_3^-, (b) SO_4^{2-} and (c) NH_4^+. The rainwater concentrations are shown as follows: (a) NO_3^-, blue; (b) SO_4^{2-}, red; and (c) NH_4^+, orange (line and triangles). Time series of the NO_3^- (blue), SO_4^{2-} (red) and NH_4^+ (orange) concentrations in the rainfall (lines and triangles) and in the air (lines) (d).

Figure 2. Time series of particle number size distributions (a) are measured by POPC, SPAMS (take SO$_4^{2-}$ for example) and SMPS, respectively. The averaged spectrum distribution of number concentration during the APHH-Beijing campaign (a) for SMPS (purple line), POPC (green line) and NO$_3^-$ (blue line), SO$_4^{2-}$ (red line) and NH$_4^+$ (orange line) by SPAMS.

Figure 3. Multimethod estimation of the BWSCs.

Atmospheric
Chemistry
and Physics
Discussions

Open Access

EGU

490

Figure 4. Multimethod estimation of the BWSCs and comparisons with previous studies.
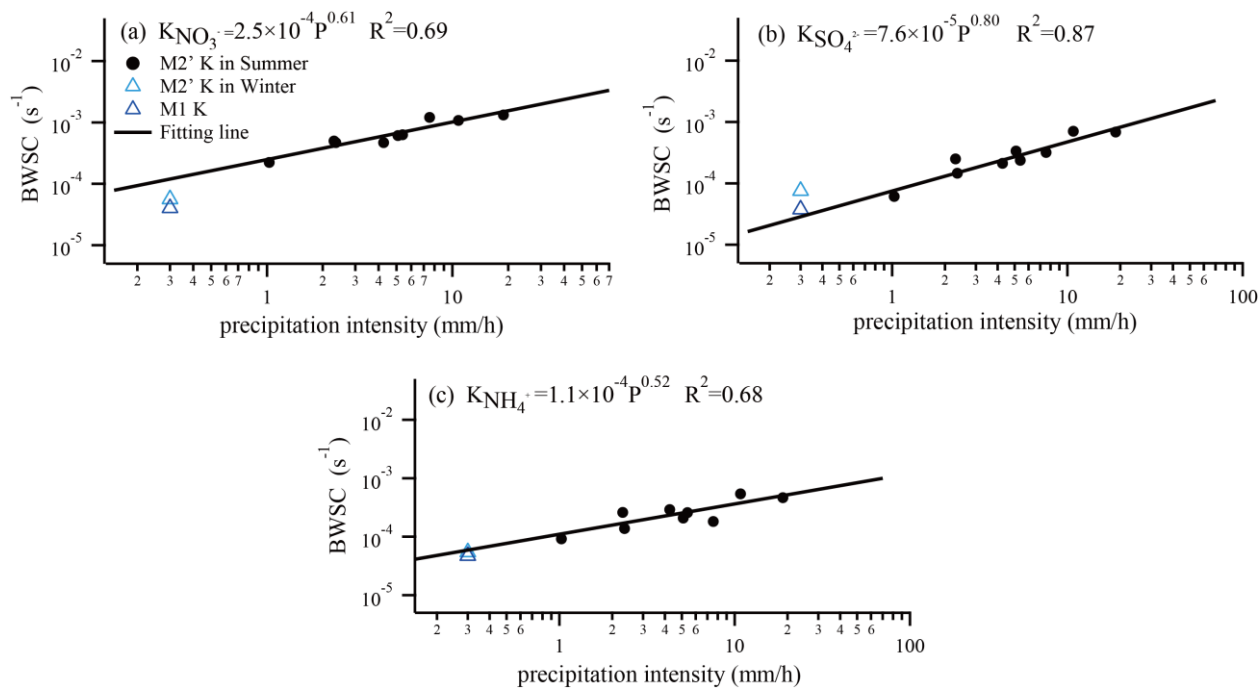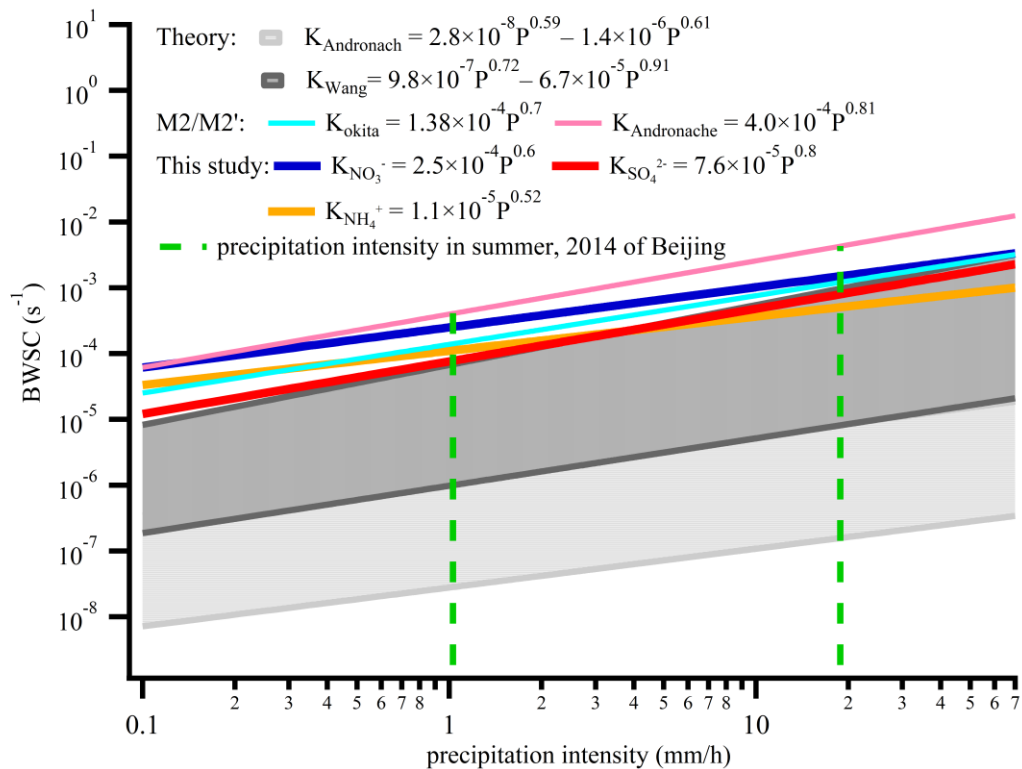
Figure 5. Scatter plots of the BWSCs and precipitation intensity for NO_3^- (a), SO_4^{2-} (b) and NH_4^+ (c) (black dots: M2' in summer by Xu et al. (2017), light blue triangle: M2' in this case, deep blue triangle: M1).

Figure 6. The parameterization of BWSCs with the rainfall intensities.

495